A PULSE FORMING NETWORK DESIGN FOR ELECTROTHERMAL-CHEMICAL COMBUSTION CHARACTERIZATION OF SOLID PROPELLANTS

M. Del Guercio, I. Stobie, G. Katulka, W. Oberle
US Army Research Laboratory
Weapons Technology Directorate
Aberdeen Proving Ground, MD 21005-5066

ABSTRACT

The combustion of solid propellants subjected to plasma augmentation, has been studied with a 300 kJ maximum stored energy pulse forming network (PFN) in the range of 1 kJ/g of electrical energy over a 1.2 ms pulse length. A closed chamber vessel is used for the combustion of these solid propellants in which the plasma is injected via a plasma generator. To characterize the effects of such plasma augmentation on propellant combustion over a longer pulse length, this PFN was upgraded to a maximum stored energy output of 400 kJ with a 2.4 ms pulse length. This report discusses the theoretical calculations, PFN upgrade design and fabrication details. Also provided are the design and modifications of the plasma generator that allows a delayed plasma injection with respect to the propellant ignition. Details of the plasma delay firings are also discussed.

INTRODUCTION

A closed chamber study in the combustion of solid propellants, subjected to plasma injection has been conducted at ARL using a 129.4 cc closed vessel with an electrode assembly that includes a plasma generator and an erosion nozzle (Fig. 1a). A lumped element transmission line pulse forming network (PFN) with a 300 kJ maximum energy output powered the injector. It provided a pulse length of 1.2 ms and was operated in the range of 20 kJ per 20 g of propellant (1 kJ/g energy density). The need to characterize the effects on propellant combustion of longer plasma injection duration (2.4 ms), motivated the PFN upgrade to be described. The modifications included the addition of two capacitors and additional buswork, damping resistors, and eight new inductors(Fig. 2a). Design and fabrication aspects of the induction coil construction are detailed as well as the plasma generator design changes, which were implemented as tests progressed. The plasma delay firings dictated the implementation of an amplifying pressure-voltage detector whose function is to trigger the PFN after the conventional ignition of the propellant occurs(electric match ignition) and before its maximum pressure is reached. Discussion of this circuit and its integration to the hardware is also covered, as well as the results of the plasma delay firings.

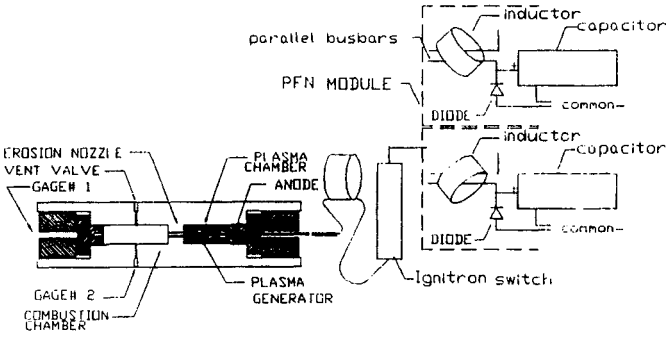

Figure 1a. Closed Chamber and Plasma Generator

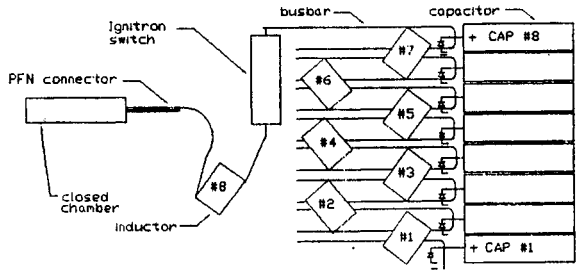

1b. 2.4ms PFN schematic

PFN MODIFICATIONS

Through circuit analysis using the code Microcap it was determined that adding two more 830 μF capacitors to the six in use in the original PFN plus a change to eight 30 μH inductors, would most economically extend the 1.2 ms pulse length to the 2.4 ms desired providing an output impedance close to the 100 mΩ value of the load, and so maximizing the power transfer into it. The 1.2 ms pulser is schematized in Fig 2a. The current and voltage profiles(Fig. 2b) of the 1.2 ms pulser fired at initial charging capacitor voltage of 5 kV (corresponding to 60 kJ of stored energy) show the pulse length. Figure 3a shows the schematic of the 2.4 ms pulser and Figure 3b, the simulated 100 mΩ resistive load tests at 5 kV Vin.

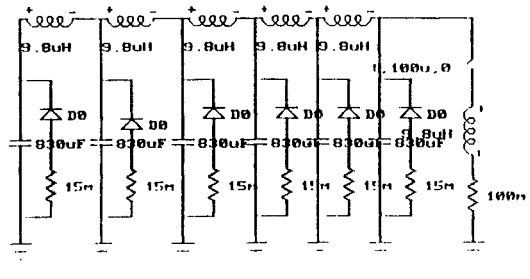

Figure 2a. 1.2 ms Pulser

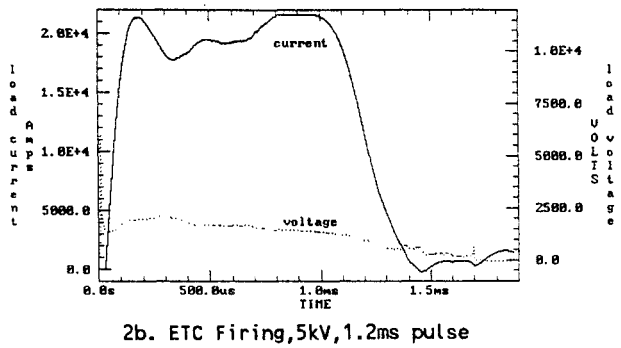

2b. ETC Firing,5kV,1.2ms pulse

Report Documentation Page

Form Approved
OMB No. 0704-0188

1. REPORT DATE	2. REPORT TYPE	3. DATES COVERED
JUL 1995	**N/A**	**-**

4. TITLE AND SUBTITLE
A Pulse Forming Network Design For Electrothermal-Chemical Combustion Characterization Of Solid Propellants

5a. CONTRACT NUMBER
5b. GRANT NUMBER
5c. PROGRAM ELEMENT NUMBER

6. AUTHOR(S)

5d. PROJECT NUMBER
5e. TASK NUMBER
5f. WORK UNIT NUMBER

7. PERFORMING ORGANIZATION NAME(S) AND ADDRESS(ES)
US Army Research Laboratory Weapons Technology Directorate Aberdeen Proving Ground, ND 21005-5066

8. PERFORMING ORGANIZATION REPORT NUMBER

9. SPONSORING/MONITORING AGENCY NAME(S) AND ADDRESS(ES)

10. SPONSOR/MONITOR'S ACRONYM(S)
11. SPONSOR/MONITOR'S REPORT NUMBER(S)

12. DISTRIBUTION/AVAILABILITY STATEMENT
Approved for public release, distribution unlimited

13. SUPPLEMENTARY NOTES
See also ADM002371. 2013 IEEE Pulsed Power Conference, Digest of Technical Papers 1976-2013, and Abstracts of the 2013 IEEE International Conference on Plasma Science. Held in San Francisco, CA on 16-21 June 2013. U.S. Government or Federal Purpose Rights License

14. ABSTRACT
The combustion of solid propeLLants subjected to plasma augmentation, has been studied with a 300 kJ maximum stored energy pulse forming network (PFN) in the range of 1 kJ/g of electrical energy over a 1.2 ms pulse Length. A closed chamber vessel is used for the combustion of these solid propellants in which the plasma is injected via a plasma generator. To characterize the effects of such plasma augmentation on propellant combustion over a Longer pulse Length, this PFN was upgraded to a maximum stored energy output of 400 kJ with a 2.4 ms pulse Length. This report discusses the theoretical calculations, PFN upgrade design and fabrication details. ALso provided are the design and modifications of the plasma generator that allows a delayed plasma injection with respect to the propellant ignition. Details of the plasma delay firings are also discussed.

15. SUBJECT TERMS

16. SECURITY CLASSIFICATION OF:			17. LIMITATION OF ABSTRACT	18. NUMBER OF PAGES	19a. NAME OF RESPONSIBLE PERSON
a. REPORT	b. ABSTRACT	c. THIS PAGE			
unclassified	**unclassified**	**unclassified**	**SAR**	**7**	

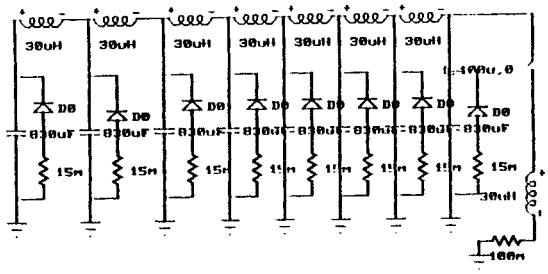

Figure 3a. 2.4 ms Pulser

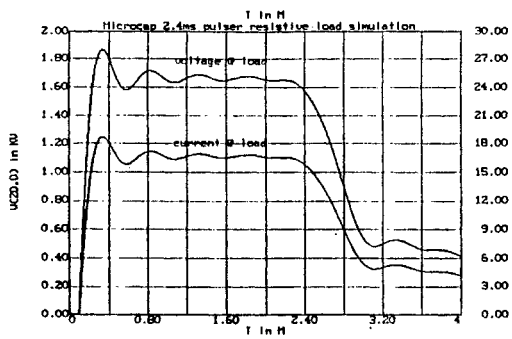

3b. Microcap Simulation.

DESIGN CRITERIA

The problems faced in this upgrading included installing eight coils in the space formerly occupied by six coils and providing the added support for their increased weight. This had to be done while retaining the design criteria of the earlier design:

a) arrange adjacent coils'axes at right angles and strive for the greatest separation to minimize mutual coupling, which is difficult to calculate and achieve accurately.

b) maintain greatest separation between coils and field-sensitive Ignitron and diodes.

c) orient the diodes so that their currents do not interact with the magnetic fields of the parallel plate bus and force non-uniform diode current distributions.

d) orient all coils so that their fields would have least effect on diodes.

The earlier bus work was utilized in the upgrading. Some parallel plate extensions were added to provide the desired positioning of the inductors. The resistance of the bus bars is a function of the depth "δ" to which the current has penetrated the aluminum (ie., at which the current density has reached avalue of 1/e of the current density at the surface) and this, in turn, is a function of time. The skin depth equals:

$$\delta = \sqrt{(1/\pi f \sigma \mu)}$$

approximately 2.6mm at 1 kHz; where the aluminum conductivity σ = 3.82x10E07 mhos/m, and $\mu = \mu 0 \mu r$; where μ_0 = 4πx10E-07 H/m and μr= 1.00002 the permeability of free space and of aluminum respectively. The skin depth (δ) will increase as the pulse width increases. The resistance of the conductors may then be approximated by:

$$R = l/(\delta w \sigma);$$

"l" being the length of the conductor and "σ", the conductivity of aluminum and "w" the conductor width. The conductors were then made of 0.635 cm thick aluminum plate, machined with round edges to a width "w" of 12.7cm; in the extensions they are spaced 2.54 cm apart, center to center. To keep the inductor field away from the crowbar diodes, the Ignitron switch was not located at the end of the circuit, as that would force the last inductor closer to the diode pack. Each bus bar has "U" shape(Figure 1b), lying horizontally and away from the capacitor, and connected to it at its middle point. All inductors are then connected in series, while all capacitors are connected in the legs of a "π" configuration(Figure 3a).

INDUCTANCE AND STRESS CALCULATIONS

The number of turns required to obtain an inductance L of 30-uH on a 15.3"diameter form, was determined using Nagaoka's formula[1] and its tabulation for the constant K.

$$L = 0.004\pi^2 N^2 (a^2 K/b)\ \mu H \qquad (1)$$

a being radius (cm) measured from center of the coil, to the center of the conductor; b the center to center length of the winding (approx. tube length), K is a function of the b/2a ratio and N the number of turns. A computer program was written which started with an estimate of the number of turns needed. The program determined the winding length required by the insulated wire, and then interpolated the table in reference (1) to find the corresponding values of K. The formula then produced a new value of N, and a new length. The interpolation, then found a new K value. This process was repeated iteratively until values of N, b and K converged to a sufficiently constant and consistent set. It then computed the outside dimensions of the physical space occupied by the coil and the D.C resistance of the winding and its corresponding L/R decay time. The program calculated the radial bursting force for a given value of current i. This routine recognized that the expansive force developed by current flow in a coil may be determined by equating the change of electromagnetic energy in the coil to the mechanical work done in expansion $\Delta E = F.\Delta a$

The energy stored in a coil is

$$E = (1/2)Li^2 \qquad (2)$$

Equation 1 relates the coil's inductance to its physical dimensions; when an increase in its radius a causes its inductance to increase (as given by the derivative):

$$\Delta L/\Delta a = 0.0395(N^2/b)(2aK + a^2 \Delta K/\Delta a) \qquad (3)$$

Then the change in energy (for an unchanging current) would be

$$\Delta E/\Delta a = (1/2)i^2 \Delta L/\Delta a \qquad (4)$$

Since, for a mechanical system $\Delta E = F_r . \Delta$ (5)
by solving for radial force F_r and substituting from Equation 4, we find
$F_r = (1/2) i^2 [0.0395 (N^2/b)(2aK + a^2 \Delta K/\Delta a)]$ (6)

The computer calculated $\Delta K/\Delta a$ for the tabular interval containing K, and produced an estimate of the radial force distributed over the entire winding. This force distribution was assumed uniform and as a radial force F_r/l per unit length, and in analogy with the three dimensional method of computing hoop, or tangential stress in a pressure vessel, the tangential component of this radial force per length was integrated over the length of a 1/4 turn of the coil, to obtain the tension force F_r in the conductor.

$$F_t = \int_0^{1/4} \frac{F_r}{l} \sin\theta dl = \frac{F_r}{l} \int_{\pi/2}^{0} R \sin\theta d\theta = \frac{F_r R}{l}$$

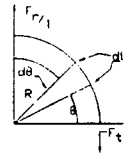

When this force is divided by the wire cross section, it approximates the tensile stress tending to break the copper winding. This stress should not exceed a safe value for copper. Under normal operating conditions our design indicated large margin of safety. However, in the case of catastrophic failures (capacitor breakdown, buswork arcs to ground, arcs across load, etc) currents may rise to excessive levels, and Kevlar 29 cloth wraps were used to add strength. The effective thickness T_e of the #352 Clark-Schwebel cloth used, was approximated by dividing the published weight per unit area of the cloth by the published density of the Kevlar 29.

$T_e = (1.767E\text{-}01\ kg/m^2) / (1.439E03\ Kg/m^3) = 1.23E\text{-}04\ m$.

The cloth is nominally 0.254 mm thick, so 48% was used as the packing density of the threads. Each turn on the coil occupies 32.8 mm of coil length and, so, is covered by this width of cloth. The urethane potting compound (Hysol XVS-0104) encasing the coil, should distribute applied force over the whole area of the Kevlar cloth. The calculated tangential force of 20612 N for a 100 kA discharge, produces a stress of 153 MPa in the copper wire, and may stretch it. If this force is transferred to the cloth, the stress induced equals force divided by cross section. The cross section is the product of:
packing density x width x packing density x thickness

$0.48 \times 3.28E\text{-}02\ m \times 0.48 \times 2.54E\text{-}4\ m = 1.92E\text{-}06\ m^2$

The stress is : 0.0206 MN / 1.92E-06 m^2 = 10700 MPa, which is three times 3625 MPa, the maximum stress for Kevlar. Consequently four layers of cloth were wrapped around the coil prior to potting.

COMPONENT MODIFICATIONS

The demand that the pulse length which is proportional to $\sqrt{(LC)}$ be increased, while the line's characteristic impedance which is proportional to $\sqrt{(L/C)}$ was maintained at its power-maximizing match to the 100 mΩ capillary impedance, dictated the total inductance L and the total capacitance C increase by the same factor. Doubling the size of the six coils to 20 μH and using twice the number of 830 μF capacitors would have worked, however neither the added six capacitors nor the space for them was available. The above compromise was selected because its large excess of available energy, in spite of its impedance mismatch which was less critical than the pulse length desired. The eight 30 μH coils and two 830 μF capacitors were used as in previous Fig. 3a. The resulting 2.4 ms pulser's characteristic impedance of 190 mΩ did not match as expected the 100 mΩ impedance of the plasma's capillary, but the modified PFN design turned out the desired pulse length with a maximum stored energy of 400 kJ (eight capacitors each rated at 11 kV storing up to 50 kJ). Later resistive tests demonstrated that the pulser's efficiency remained in the 70% range.

The total capacitance was increased from 4.98 mF (830 μF x6) to 6.64 mF (830 μFx8), and the total inductance, from 60 μH (6x9.8 μH) to 240 μH (8x30 μH). Two additional resistances, in series with the crowbar-diodes which impede voltage reversal in the caps, were manufactured as the previous ones, utilizing a Nichrome strip 914 mm by 76 mm in an inductance lowering zig-zag configuration. These resistors by limiting the current through the expensive crowbar diodes, protect them from damage should the load become a short circuit. Their impedance value of 15 mΩ was found adequate through a Microcap simulation. All connecting buswork to and from the inductors was secured, at one foot intervals approximately, by G-11 clamps to counter the magnetic pressure produced by the high currents flowing in and out the inductors and tending to separate the bus bars. The limited space within the range constrained the diameter for the new inductors to about 406 mm, and the maximum length to 330 mm. Also, as the magnetic flux linkage between adjacent coils had to be minimized, to reduce the mutual inductance, a 90 degree angle was desired between their axes, complicating their placement even further.

INDUCTOR FABRICATION

Each of the eight inductors was wound on a plastic pipe, 305 mm long, of 389 mm OD and 11.2 mm thick walls. A 15.9 mm O.D, rubber insulated, 2/0 AWG copper welding cable, 20.5 meters long was folded in half. Its ends were passed from the inside to the outside of the coil tube, through two adjacent holes. The cable ends were then twisted with a careful controlled pitch which, when wound on the form, nested with the twists of the adjacent turns. Winding was done by hand turning a lathe, which was fitted with a dividing head. Commercial Litz wire of the required current capacity has a larger diameter, and would have required an unacceptable longer or larger diameter coil.
A two layer coil (possible of smaller volume) may experience higher stresses and has its start and finish at the same end of the form, with resulting insulation demands. The chosen configuration obtained, added conductor cross section with acceptable increase in coil length while the crude Litz effect of its twist, equalized currents in the parallel conductors.
To counter the expansive magnetic pressure on the windings, as current is pulsed through, they were tightly

wrapped with Kevlar cloth and potted in Hysol Epoxy which mechanically coupled the coil to the Kevlar in a solid casting. The Hysol consisted of two components, mixed to a 400g A, 280g B ratio, approx. Vacuum was applied to each sample mixture, up to 1.5 mm Hg, to avoid air bubbles and so, to improve the tensile and shear properties of the cured Epoxy.

CIRCUITRY

The energy "dumping" to abort the PFN charging process (Fig. 4a) or in case of a misfire, is controlled through fiber optic links. The load voltage measuring circuit is comprised of a 266 Ω resistor string (R) and the series 100 μF blocking capacitor (C) which together span the load. In times short with respect to the time constant RC, the current through the resistor is proportional to the load voltage. The lead to the resistor chain is encircled by a Pearson transformer (a Rogowski coil wound on a magnetic core, whose high L/R ratio renders it self-integrating) which senses the current and produces a proportional voltage (in this instance, 0.1 Volt/Ampere). Additional fiber optics were installed to operate a Ross high voltage relay, used for shorting a 100 μF blocking capacitor used in the voltage measuring circuit at the load, as this capacitor could become fully energized if the load opens. The current measurement at the load is done as on the previous PFN, through a Rogowski coil.

PFN TESTING

The eight modules are triggered simultaneously by one Ignitron closing switch. Solid state crow-barring protects each capacitor from voltage reversals. Because the pulse profile desired requires only one Ignitron switch, the conditions for diode damage are reduced, as the simultaneous discharge of the capacitors decreases the chances of large di/dt or high reverse dV/dt across the conducting crow-bar diode (Katulka et al. 1994). Resistive load test current and voltage for the 2.4ms pulser at 3kV charging voltage are shown in Fig. 4b.

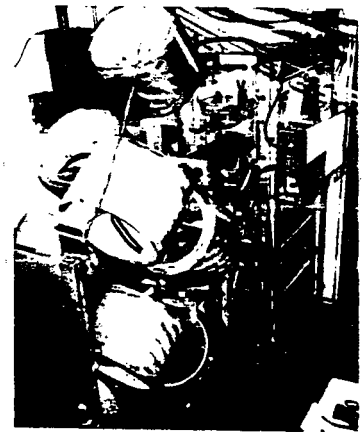

Figure 4a. 2.4 ms ARL Pulser.

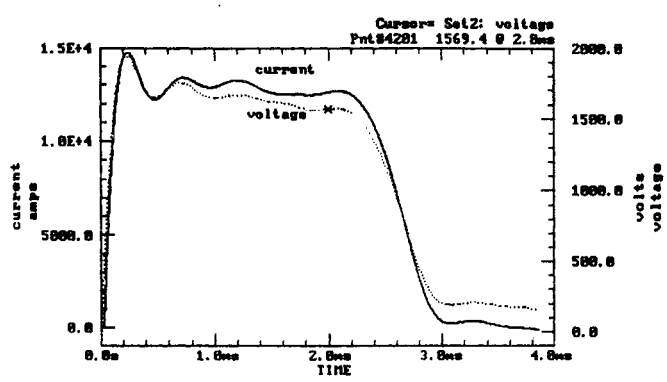

4b. 2.4ms PFN resistive load test.

As the transition from the 1.2 ms pulser to the 2.4 ms pulser was implemented,the resistive dummy load tests at 5 kV Vin revealed data acquisition noise problems (83 kJ input, 60 kJ at the load), and a short at the PFN/electrode connector. The actual ETC firings however, i.e. JA2 propellant ignited by plasma injection, revealed bonding occurring on components of the plasma injector to the plasma chamber walls, making disassembly difficult. This bonding caused erosion on the plasma chamber wall, which further complicated the chamber sealing from the propellant combustion gases. What follows is a description of the results found through inspection of the damaged components, and the reasons and theory on which the modifications were based upon.

LOAD TESTING

The PFN ETC setup has the electrode-chamber head and E-glass liner-nozzle assembly inserted into the vessel's plasma chamber, with the electrode end, protruding about an inch through a heavy retaining nut, which impedes the chamber head from expulsion. On the previous 1.2 ms pulser (300 kJ), an insulated 102 mm long copper connector secured the electrode end to the PFN output and provided the path for the PFN discharge. The PFN output consisted of a 38.1mm OD of solid copper tube, threaded in one end to accept the electrode end, and welded to the last inductor output wires on the opposite end. During resistive load tests at 3 kV with the 2.4 ms pulser (400 kJ), a short was observed between the flat area of the retaining nut and the exposed frontal area of such copper tube (PFN output). For this reason, several layers of dielectric protected by heat shrinkable tubing, were added around a new 204 mm extended copper connector.
The PFN output copper tube was also insulated in its totality, leaving exposed only the holes for the electrode tightening screws. Measurements made for di/dt and voltage at the load for the 2.4 ms PFN resistive test, became unusually noisy using over 3 kV of voltage input. A short occurring at the 3 kV resistive load test, between some of the capacitor casings and the bus bars, were suspect as the cause for this noise. Mylar sheets (0.127-mm thick) were inserted in between, and all previous noise was eliminated from di/dt and voltage fiber-optic acquired signals, even at higher voltages (5 kV).

CLOSED CHAMBER ETC FIRINGS

A series of four firings AT 5kV were conducted to test the performance of the plasma generator assembly, and to determine what was the effect of the firings on the component parts and vessel's walls. This was a major concern due to the increase in pulse length as well as the increase in energy. The vessel and plasma chamber set up are shown in Fig.7 and instrumentation set up in Fig.8a.

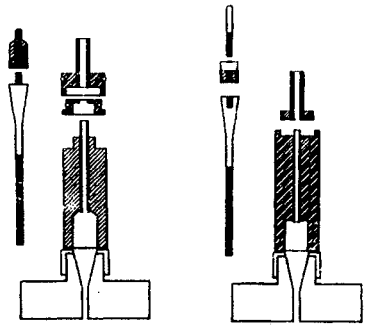

Figure 5a. 5b.

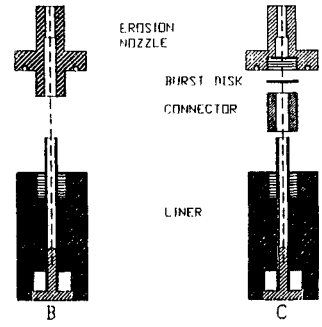

Figure 6.

First ETC Firing.

A short ocurred between the insulated conical section of the electrode(Fig. 5a), which seats on the chamber head area of the same shape and the chamber head. As this assembly is hi-potted and tested, the cause was assumed to be damage sustained on the insulation during the firing, due to hot gases leaking between the electrode tip and liner towards the insulated part of the electrode. The electrode tip used in this shot is shown in Fig. 5a.

Second ETC Firing

Using the same plasma generator configuration, this shot however, bonded the nozzle sides to the vessel's wall. A high energy arc was suspected as the cause, and damage to the nozzle and vessel's walls was extensive(Fig. 5a)

Third ETC Firing

The electrode used for this shot had a hollow tip(Fig. 5b) which deforms as pressurized by the gases traveling downwards through the capillary, sealing the capillary and protecting the electrode insulation. This design proved effective in protecting the insulation, solving the problem of a short circuit, as ocurred at the first ETC firing.

Fourth ETC Firing

For this firing, the nozzle was enbeded in the liner with the purpose of avoiding the nozzle sides from bonding to the vessel's walls. However, this design failed in keeping the plasma confined to the capillary, as residues escaped into the plasma chamber.(Fig. 5b)

NEW NOZZLE DESIGN

Due to the problems encountered with these previous design, a solution had to be found to eliminate the bonding and heavy erosion problems to the vessel's walls, as well as the excessive amount of metallic residues deposited on the plasma chamber walls, a fact that forced the stopping of operations to get the chamber properly clean and fit for the on going tests.

A new type of nozzle(Fig. 6,B) was then used for an ETC test, at 3 kV charging voltage in a 50 cc vented chamber. This shot showed that no leaks ocurred at the E-glass liner and nozzle joint, and that neither metallic residues bonded any of the plasma generator components unto the plasma chamber as before. This design(Figure 6b), shows a nozzle threaded at its base which preloads a sealing "O" ring as is screwed into the E-glass liner. This provides an effective seal to the capillary plasma and gases from leaking into the plasma chamber. This nozzle and liner configuration was then selected for the plasma delay firings.

PLASMA DELAY FIRINGS

A variation of the design discussed previously was used(Fig. 6, C). The material for the burst disk which protects the nickel wire from being blown away by the propellant pressure was first selected from a 0.03" thick aluminum sheet. The vessel and plasma delay set up are shown in Fig. 9b and instrumentation set up in Fig.8b. The current pulse for the 1.2 ms pulse length PFN configuration, which is the one chosen for the plasma delay injection, takes an average of 200 μs from initiation to peak, while the delay for the pressure rise to peak is about 50 μs from the current pulse completion time(this pulse length was obtained by using only 4 banks). It was also observed that during ETC firings, the transducer pressure trace rises after the current peaks, and reaches its maximum value when the electrical input is completed. This implies that the transfer of energy from the PFN to the combustion chamber has a total delay of about 250 μs. The energy transfer does end after 1.2 ms, which is in agreement with the analytically calculated energy and current profile for this 1.2 ms pulse configuration. The sequence for the plasma-delay injection first starts with the conventional ignition of the propellant in the vessel's propellant combustion chamber. It ends with the electrical energy being injected in the 5-cm^3 plasma capillary chamber(Fig. 9b)of the E-glass liner, contained in the plasma chamber, at the opposite end of the vessel(PFN side). The plasma initiated by the PFN discharge transfers the energy to the already ignited propellant during its later portion of pressurization. An amplified pressure signal from a transducer located at the vessel, senses the igniting propellant and enables a voltage detector circuit(via fiber-optic link) to trigger a time delay generator

which subsequently triggers the PFN switch at very early stages of the propellant pressure profile. This set up allows the determination of the best time frame for the plasma injection and electrical energy injection optimization. The 250-μs delay mentioned before, which included the 50-μs delay in the plasma pressure injection and detection, had to be accounted for if a preset an additional time delay was to be added between the conventional ignition and the injection time of the plasma, so the total and final delay is less than the time the propellant takes for to complete its pressurization.

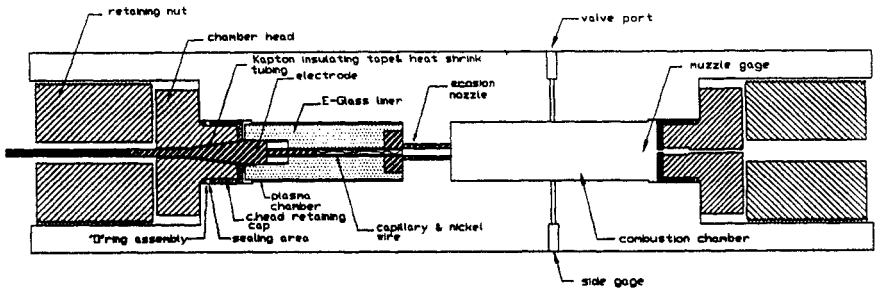

Figure 7.

PLASMA DELAY SET UP

For plasma delay firings the vessel's muzzle gage is replaced by a chamber head and steel electrode set up, to accommodate the electric match that initiates the conventional ignition of the propellant inside the 120 cm^3 combustion chamber(Fig.9b). A Kistler quartz pressure transducer(model 607C4) which is installed in the lateral gage cavity of the vessel(Fig 8b) and a Kistler Dual Mode Voltage Charge Amplifier(model 5004), feed a fiber-optic link, consisting of a transmitter (Dymec model 6723) and a receiver(Dymec model 6722), transfers this signal from the range to the voltage sensor(Fig.9a). This approach enables the triggering of the PFN to be a function of the particular pressure rise profile of the propellant, as the amplifying voltage detector(Del Guercio et al. 1994), with a delay of less than 1 μs outputs over 3 V with a minimal input signal of 400 mV, which corresponds to about 1/20 of the propellant maximum pressure rise, or less than 20 MPa (8.0 V calibrated output or 50,000 psi maximum).

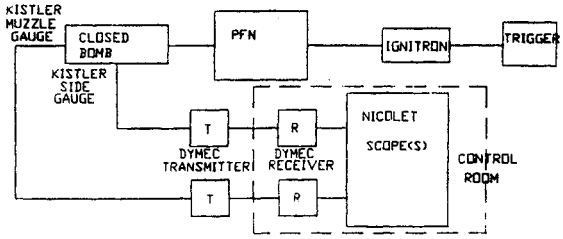

Figure 8a. ETC instrumentation set up

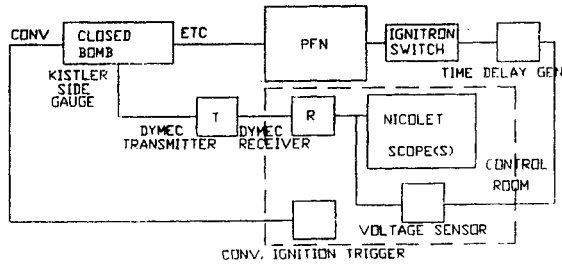

8b. ETC /Plasma Delay instrumentation set up

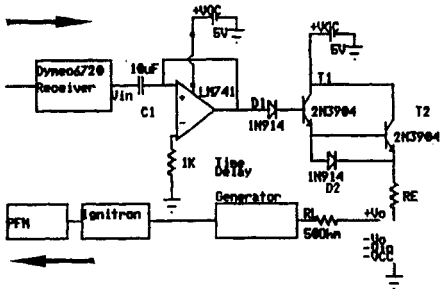

Figure 9a. Voltage sensor/amp

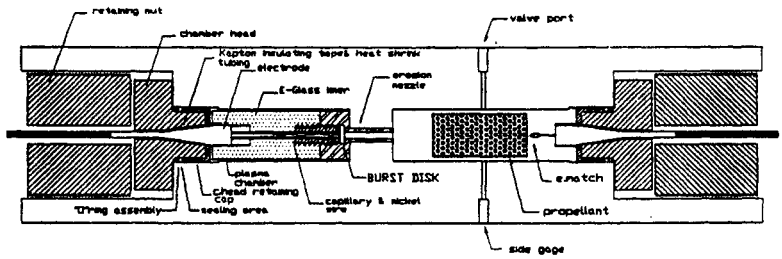

9b.

First Plasma Delay Firing.

The propellant chosen had a raise time to maximum pressure of 7ms approximately. The plasma then had to be injected before this maximum pressure occurs, as a necessary condition to alter the burning rate of the

propellant. The time delay chosen was 5ms, as at that time the propellant pressure would shear the 0.03" thick aluminum disk at the exposed area left by the nozzle. The charging voltage selected was 3kV. The plasma was formed but its discharge did not happen through the nozzle channel into the combustion chamber, but it perforated the nozzle from the inside across to the stem part of its base. Only the later or decaying portion of the propellant pressure curve was recorded by the scopes, and the current and voltage profiles at the load indicated only half of the energy expected were injected into the plasma generator. Due to the extensive damage caused to the nozzle (Fig.6,C), previously used and available type(Fig.6,B) were used, which shorted the capillary by a length equal to the threaded part of the nozzle once the burst disk is placed at its base against the liner.

Second Plasma Delay Firing.
The burst disk was compressed between the liner and the base of the nozzle. The generation of the plasma was apparently affected by the preceding propellant combustion and chamber pressurization as the scopes only recorded a DC voltage apparently across the PFN spark gap, while there was no di/dt. Inspection of the liner and plasma generator indicated that the burst disk was destroyed.
Because of this problem, a non delay ETC firing was conducted, to check on the effects of the shortened capillary. Data recorded indicated that di/dt, voltage as well as energy were as expected, and that the plasma injection was not adversely affected. However, a weaker plasma could be adversely affected by the pressure of the burning propellant, causing its extinction, and so impede the injection of energy across the plasma generator.

Third Plasma Delay Firing.
The pressure indicated as expected a second rise after its maximum, due to the plasma injection. However voltage and di/dt traces were similar as that of the second firing.
At this time the results are inconclusive and more firings are planned with the original nozzle type(Fig.6,C).

CONCLUSIONS

The modified pulser performed as expected , raising the energy of a typical ETC firing at 5kV input, from 35 kJ to 60 kJ. The outputs of current and voltage verified that minimal coupling if any, occured between the inductors and that the 90 degree tilting was effective. The new design for the ETC nozzle(Fig. 6,B)) worked successfully. The plasma delay nozzle design(Fig.6,C) failed due to the plasma perforating the base of the nozzle stem, so a thicker wall will ensure the plasma injection through the inner nozzle channel. This fact together with the proper capillary length could ensure a successful plasma delay test.

REFERENCES

Del Guercio M., Katulka G.L. and Fortier S., Electronic and Fiber-Optic Applications in Pulsed Power Networks, ARL-TR-404, May 1994.

Del Guercio M.,H. Burden, I. Stobie, K. White, G. Katulka and S. Driesen.,"Pulse Forming Network in the ETC Combustion Characterization of Plasma Augmented Solid Propellants", 31st JANNAF Combustion Subcommitee Meeting, Lockheed Missiles and Space Company, Sunnyvale, CA, October 1994.

Grover, F.,Inductance Calculations, Working Formulas & Tables. Triangle Pk NC, Instrument Society of America, 1982.

Katulka G.L., Burden H., Zielinsky A., White K., "Electrical Energy Shaping for Ballistic Applications in Electrothermal-Chemical Guns," Vol 1, CPIA Pub 557 pp. 339-347, November 1990.

Oberle W. Private Communication, U.S. Army Research Laboratory, Aberdeen Proving Ground, MD, 1994.

Oberle W., "BRLCB: A closed-chamber Data Analysis Program, . Part I: "Theory and Users's Manual"; Part II: "Theory and User's Manual". ARL-TR-36, U.S army Research Laboratory, Aberdeen Proving Ground MD, January 1993.

Oberle W., Stobie I., DelGuercio M. and White K., "Analysis of Plasma-Augmented Burn Rates of JA2 Propellant," 31st JANNAF Combustion Subcommittee Meeting, Lockheed Missiles and Space Company, Sunnyvale, CA, October 1994.

White, K., Oberle W., Juhasz A., Stobie I., K. Nekula, Katulka G.L., and Driesen S., "Combustion Control Requirements in High Loading Density Solid Propellant ETC Gun Firings," 31st JANNAF Combustion Subcommittee Meeting, Lockheed Missiles and Space Company, Sunnyvale, CA, October 1994.